Quantum Electronics **47** (8) 705–710 (2017)

CONTROL OF LASER RADIATION PARAMETERS https://doi.org/10.1070/QEL16416

Offner stretcher for the PEARL laser facility

A.S. Zuev, V.N. Ginzburg, A.A. Kochetkov, A.A. Shaykin, I.V. Yakovlev

Abstract. **As part of upgrading the PEARL laser facility, a new, femtosecond Ti:sapphire master oscillator with a centre wavelength of 910 nm and an emission bandwidth of 40.5 nm has been incorporated into its scheme. To produce a new stretcher matched to the compressor of PEARL, we have carried out a comparative analysis of Martinez and Offner stretcher configurations with spherical and parabolic mirrors. The residual dispersion in the stretcher–compressor system has been evaluated using an unconventional approach based on calculation of a zero-dispersion stretcher. In experiments using the Ti:sapphire laser, a new stretcher in the Offner configuration with spherical mirrors and a compressor, we have obtained pulses of 36-fs duration, which is considerably shorter than the current pulse duration in PEARL.**

Keywords: *femtosecond pulses, ultra-high power lasers, chirped pulse stretchers and compressors, zero-dispersion stretcher, polyethylene terephthalate.*

1. Introduction

One way of raising the peak power of laser pulses is by reducing their duration. Even at a moderate energy of 10–20 J, a record high power level can be achieved. A number of petawatt lasers with pulse durations no longer than 30 fs have already been demonstrated [1–4].

In state-of-the-art ultra-high power laser systems based on chirped pulse amplification (CPA), the output pulse duration is typically determined by the emission spectrum of a femtosecond master oscillator (FMO), the gain band of the system and the transmission band and the accuracy of the dispersion match of the stretcher–compressor pair [5]. Clearly, with the advent of sources of ultra-short pulses with a shorter duration (broader lasing spectrum), it is promising to upgrade the front end of ultra-high power laser systems. In this context, like in designing a new CPA system, one is confronted with the problem of optimising the stretcher configuration. Possible configurations for each particular laser facility are analysed with allowance for its inherent features [6–9].

The pulse duration of PEARL (PEtawatt pARametric Laser), a subpetawatt laser facility [10] based on optical parametric chirped pulse amplification (OPCPA) with frequency conversion, is 45–50 fs. This value is due to the use of a Cr:forsterite laser with a centre emission wavelength of ~1250 nm as an ultra-short pulse source. An FMO pulse of ~40 fs duration is stretched in a prism–grating stretcher [11] and injected into the first stage of a parametric amplifier. Its other stages amplify the collimated ~910-nm light resulting from three-wave interaction (pump wavelength, 527 nm). The pulse is then compressed in a Treacy four-grating compressor. The stretcher and compressor of the PEARL facility are dispersion-matched up to the fourth order inclusive. Note that the fifth-order dispersions in these devices do not cancel each other but add up, thus increasing the pulse duration.

Currently, the front end of PEARL is being upgraded, because Avesta Project Ltd. (Russia) has created a Ti:sapphire laser with a centre emission wavelength of 910 nm and a spectrum corresponding to a transform-limited pulse duration of 30 fs. For OPCPA with a Ti:sapphire FMO, a classic stretcher–compressor phase matching condition differing from the previous one should be met, because in the new configuration both dispersion devices will have the same operating wavelength. The new configuration should ensure a better matching between these devices in terms of the compensation for the residual higher order dispersion in comparison with the existing configuration.

In this paper, we report the development and properties of a new stretcher for PEARL.

2. Spectral and temporal characteristics of the Ti:sapphire laser output

The femtosecond Ti:sapphire laser specially designed for the front end of PEARL generates ultra-short pulses of ~56 s duration with a centre wavelength of 910 nm and ensures an average output power of up to 400 mW. The measured full width at half maximum (FWHM) of the laser emission spectrum, 40.5 nm, corresponds to a transform-limited Gaussian pulse duration of 30 fs, which is almost a factor of two shorter than that measured with an AA-20DD autocorrelator (Avesta Project, Russia).

To evaluate the uncompensated dispersion in the Ti:sapphire laser and examine the feasibility of pulse compression to the shortest possible duration, we carried out experiments

A.S. Zuev, V.N. Ginzburg, A.A. Kochetkov, A.A. Shaykin Institute of Applied Physics (Federal Research Centre), Russian Academy of Sciences, ul. Ul'yanova 46, 603950 Nizhnii Novgorod, Russia; e-mail: ya.al.zuev@yandex.ru;
I.V. Yakovlev Institute of Applied Physics (Federal Research Centre), Russian Academy of Sciences, ul. Ul'yanova 46, 603950 Nizhnii Novgorod, Russia; Lobachevsky State University of Nizhnii Novgorod, prosp. Gagarina 23, 603950 Nizhnii Novgorod, Russia; e-mail: ivan@ufp.appl.sci-nnov.ru

Received 2 May 2017
Kvantovaya Elektronika **47** (8) 705–710 (2017)
Translated by O.M. Tsarev

using chirped dielectric mirrors (UltraFast Innovations GmbH, Germany) and a set of K8 glass plates of various thicknesses. The chirped mirrors for broadband light with a centre wavelength of 910 nm had a second-order (group delay) dispersion of –100 fs^2. According to reference data, the group velocity dispersion in K8 glass at this wavelength is ~36 fs^2 mm^{-1}.

After passing through the glass plates, the Ti:sapphire laser beam was reflected from the chirped mirrors and directed to an autocorrelator. The number of reflections from the mirrors was varied from 2 to 12. We also varied the number of glass plates, which were 9, 30 and 67 mm in thickness. Figure 1 shows the measured laser pulse duration as a function of additional second-order dispersion. The minimum laser pulse duration, 30.3 fs, was obtained at six reflections from the chirped mirrors. Accordingly, the uncompensated second-order dispersion in the Ti:sapphire oscillator was ~600 fs^2.

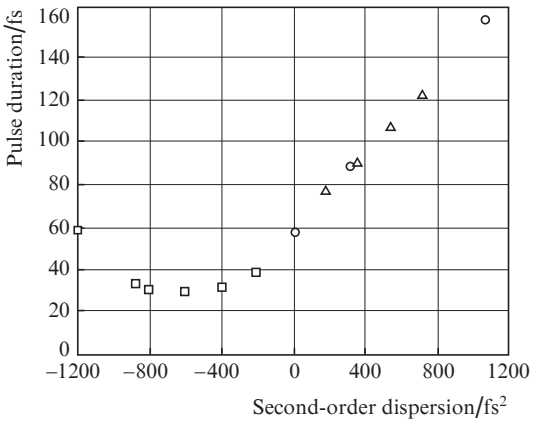

Figure 1. Ti:sapphire laser pulse duration as a function of additional second-order dispersion. The data were obtained in experiments using chirped mirrors (□), glass plates (○) and plastic plates (△).

Using the Ti:sapphire laser, we measured the linear dispersion characteristics of polyethylene terephthalate plastic at the laser emission wavelength, 910 nm. Its large nonlinearity coefficient and the possibility of producing thin, large-aperture plates of acceptable optical quality make this material potentially attractive for use in ultra-high power laser systems for nonlinear spectrum broadening to ensure additional pulse compression [12]. Polyethylene terephthalate is a new material in laser engineering, and information about its optical properties at a wavelength of 910 nm is necessary, in particular, for utilising this material in PEARL.

Plastic samples in the form of 1.5-mm-thick rectangular plates were exposed to the laser beam in front of the input of the autocorrelator. To improve sensitivity, the measurements were performed in the region where the pulse duration was a linear function of added dispersion (Fig. 1). To this end, glass plates with an appropriate second-order dispersion were placed in the path of FMO pulses. The measurements were made for one plastic plate or for two to four plates located behind each other. As a result of the measurements, the group velocity dispersion in the plastic was determined to be ~120 fs^2 mm^{-1}, which is about three times that of K8 glass.

3. Choice of the configuration and development of a new stretcher for PEARL

The use of the Ti:sapphire oscillator instead of the Cr:forsterite FMO has required developing a new stretcher, dispersion-matched to the chirped pulse compressor [13] of the PEARL laser facility. The compressor was made according to the classic Treacy configuration, using four gold-coated holographic gratings with a groove density of 1200 lines mm^{-1}. The beam was incident on the first grating at 43.13°, and the compressor base (the spacing between the gratings along the normal to their working surfaces) was 133.7 cm (146.6 cm along the ray with a centre wavelength of 910 nm).

Two main types of stretchers are commonly used in CPA/ OPCPA systems. One of them is the Martinez stretcher [14, 15], typically employed in modern systems with the use of reflective optics (concave mirrors instead of collecting lenses) [16, 17]. The other type is the Offner stretcher [18, 19], based on an Offner triplet [20], which comprises a concave and a convex mirror. The small cross-sectional size of the input beam allows for compact, single-grating, multipass stretcher configurations. In what follows, a single-grating stretcher configuration will be referred to as a four-pass system if a laser pulse impinges on the grating four times and an eight-pass system if a pulse impinges on the grating eight times.

At identical groove densities in the stretcher and compressor gratings and identical angles of incidence of light on them, we can geometrically 'add up' the schematic diagrams of these devices (Fig. 2) to give a system known as a zero-dispersion stretcher (compressor) [21]. The diffraction gratings G1 and G2 in such a system are situated in optically conjugate planes. In an ideal instance, without aberrations, light that passed through such a system and propagates in the principal plane of the device (the plane of Fig. 2) has zero second and higher order total phase dispersion, $\Phi^{(i)} = \mathrm{d}^i\Phi/\mathrm{d}\omega^i$:

$$\Phi^{(i)}_{\text{ideal zero-str}} = \Phi^{(i)}_{\text{ideal str}} + \Phi^{(i)}_{\text{ideal comp}} = 0, \quad i \geqslant 2.$$

The second and higher order dispersions of the diffraction gratings G′ and G″ (Fig. 2) and those in the G′–M1 and M2–G″ regions of the stretcher and compressor cancel each other. A zero-dispersion stretcher in which gratings G1 and G2 are situated at points A and B, symmetrically with respect to the inverting telescope (in Fig. 2, the shift of the gratings is $d = 0$), is widely used for amplitude modulation of broadband emission spectra [22, 23].

According to our studies, calculation of the zero-dispersion stretcher configuration allows one to gain information

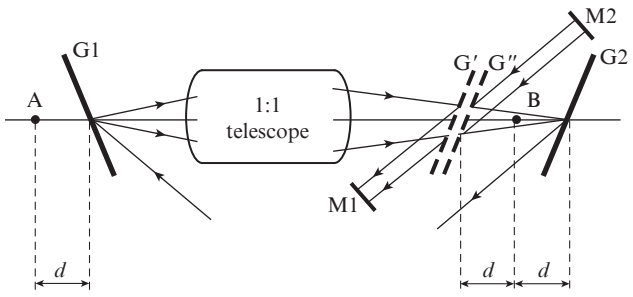

Figure 2. Schematic of a zero-dispersion stretcher (see text).

about the residual uncompensated dispersion $\Delta\Phi^{(i)}_{\text{res}}$ in a real stretcher–compressor system:

$$\Delta\Phi^{(i)}_{\text{res}} = \Phi^{(i)}_{\text{real str}} + \Phi^{(i)}_{\text{real comp}} = \Phi^{(i)}_{\text{real zero-str}} \neq 0, \quad i \geqslant 2.$$

Here, $\Phi^{(i)}_{\text{real str}}$ is the second or higher order dispersion in the region of pulse propagation from the plane of grating G1 to the plane of G′ (located symmetrically to G1 with respect to the telescope) and from the plane of G′ to mirror M1 (Fig. 2) and $\Phi^{(i)}_{\text{real comp}}$ is the phase dispersion in the regions of pulse propagation from mirror M2 to the plane of G″ and from the plane of G″ to the plane of G2. Note that $\Phi^{(i)}_{\text{real comp}}$ is not exactly the dispersion in the individual compressor because, passing through the nonideal telescope, light acquires additional angular and spatial chirps in the plane of G′ (or G″). Numerical calculations indicate that the residual dispersion in the zero-dispersion stretcher and the one in a system of a stretcher and compressor, made separately, differ by no more than 5%. In particular, for the configuration calculated by us (see below) the error of determination of the pulse duration at the output of the system does not exceed 0.5% (0.2 fs).

Possible configurations of a new stretcher for PEARL were examined using the above zero-dispersion stretcher calculation method. Stretcher–compressor match was analysed without consideration for the phase shift in the parametric amplifier stages. This approximation is justified because of the small length of the nonlinear crystals. The calculations were made in three dimensions using a ray tracing method. For zero-dispersion stretchers based on spherical and parabolic mirrors, we calculated residual dispersion as a function of a synchronous (for the gratings to remain conjugate) shift d of the gratings from their position symmetric with respect to the telescope.

Analysis of flat (two-dimensional) Martinez and Offner zero-dispersion stretcher configurations in which a ray with the centre wavelength travels along the axis of the system indicates that the second ($\Phi^{(2)}$) and third ($\Phi^{(3)}$) order dispersions in such systems are zero at any values of d. Accordingly, the residual dispersion in such systems is determined by the fourth ($\Phi^{(4)}$) and higher order dispersion. To match four-pass stretchers to the compressor of PEARL, the shift of the grating, d, along their optic axis should be 73.3 cm. In calculating $\Phi^{(4)}(d)$ (Fig. 3), to obtain compact configurations we used focal lengths of 80 cm for the concave mirrors and 40 cm for the convex mirror in the Offner stretcher. Larger focal lengths allow residual dispersion to be reduced but increase the dimensions of the stretcher.

Four- and eight-pass stretcher configurations have similar characteristic shapes of the $\Phi^{(4)}(d)$ curves (Figs 3, 4). It is seen that parabolic mirrors are unsuitable for stretchers, except in the case of very small shifts d in the Martinez configuration. The conclusion that, at small d, spherical mirrors are optimal for Offner stretchers and parabolic mirrors are optimal for Martinez stretchers was made, in particular, by Druon et al. [24]. Note that at $d = 0$ the Offner stretcher configuration is aberration-free [19], so some systems employ a dual-grating Offner stretcher in which one grating is placed at the centre of curvature of a concave spherical mirror. At the same time, aberrations in single-grating Offner stretchers with spherical mirrors are usually small [9, 17]. It is also seen in Figs 3 and 4 that the Offner stretcher has a minimum residual dispersion

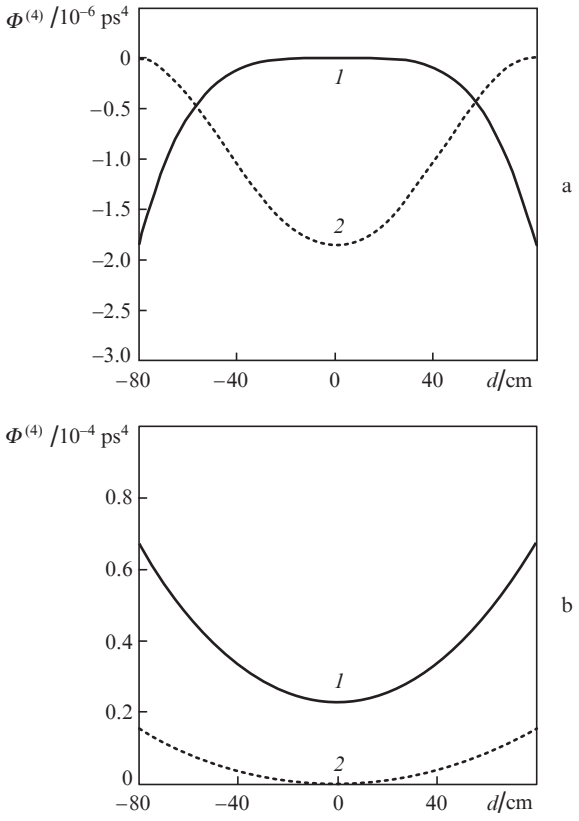

Figure 3. Residual fourth-order dispersion as a function of the shift of the diffraction grating in (*1*) Offner and (*2*) Martinez stretchers with (a) spherical and (b) parabolic mirrors with focal lengths of 80 cm for a four-pass configuration.

in a wide range of d values, so it is this configuration that is most frequently used in laser systems.

At considerable shifts of the gratings, the residual dispersion in the Offner configuration with spherical mirrors is at least one order of magnitude lower than that in the Martinez configuration with parabolic mirrors. Analysing the spherical-mirror stretcher configurations, we note that the initial point $d = 0$ (position of the first grating) is the focus of the spherical mirror in the Martinez configuration and the double focus coinciding with the centre of curvature of the mirrors in the Offner configuration. Thus, with increasing d, the first grating shifts towards the centre of curvature of the mirror in the former configuration and away from it in the latter. This accounts for the decrease in dispersion with increasing d in the Martinez stretcher configuration and the increase in dispersion in the spherical-mirror Offner stretcher configuration. It is seen in Fig. 3a that, in the configurations under consideration, for $d > 56$ cm the residual fourth-order dispersion in the Martinez stretcher is lower than that in the Offner stretcher. Thus, at large shifts d, the use of the spherical-mirror Martinez stretcher configuration may prove to be more attractive.

The use of eight-pass stretcher configurations allows more compact systems to be produced by using mirrors with a smaller cross-sectional size and smaller focal length, because the grating shift d required here is a factor of 2 smaller. For example, for matching to the compressor of PEARL, the grating shift along the optic axis of the stretcher should be

36.7 cm. Moreover, the residual phase dispersion in the eight-pass Offner stretcher configuration with spherical mirrors is substantially lower than that in the four-pass configuration with the same pulse stretching ratio (Fig. 4).

In calculations of eight-pass stretchers, we used focal lengths of 60 cm for the concave mirrors and 30 cm for the convex mirror. The calculations (Fig. 4) were performed in three dimensions for real configurations in which, to separate the input and output beams, light enters the stretcher in the plane 5 cm below the principal plane of the system. To reverse the direction of light in vertical and horizontal planes, use is commonly made of vertical and horizontal roof-mirror reflectors (VRRs and HRRs, respectively).

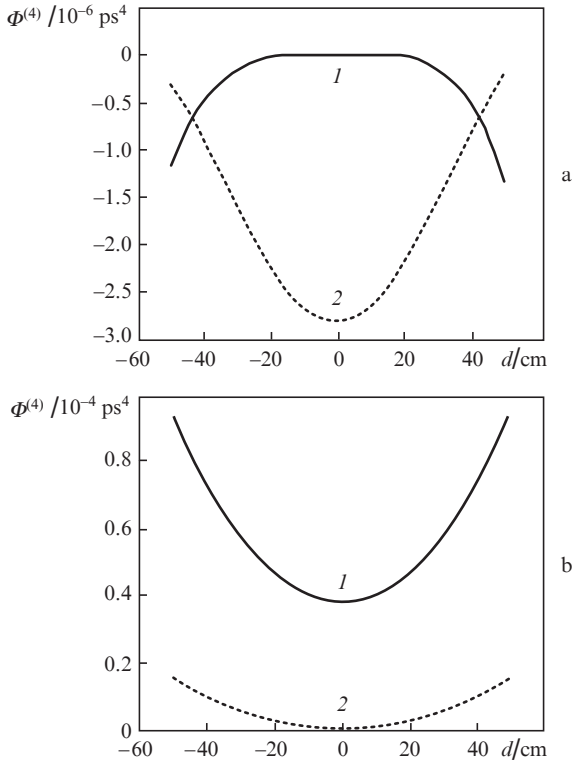

Figure 4. Residual fourth-order dispersion as a function of the shift of the diffraction grating in (*1*) Offner and (*2*) Martinez stretchers with (a) spherical and (b) parabolic mirrors with focal lengths of 60 cm for an eight-pass configuration.

Our results indicate that, unlike in the case of planar configurations, the second- and third-order dispersions are in general not zero. Nevertheless, $\Phi^{(2)}$ and $\Phi^{(3)}$ can be exactly compensated for by tilting and shifting the stretcher or compressor gratings. Thus, eventually the pulse duration and shape are determined by the residual $\Phi^{(4)}$ dispersion. In particular, our calculations indicate that the residual second-, third- and fourth-order dispersions in the spherical-mirror Offner stretcher are $\Phi^{(2)} = -2.9\times10^{-3}$ ps^2, $\Phi^{(3)} = 6.0\times10^{-6}$ ps^3 and $\Phi^{(4)} = -3.6\times10^{-7}$ ps^4. At the same time, shifting the stretcher grating by 0.9 mm and tilting it by 15″ ensures exact compensation for $\Phi^{(2)}$ and $\Phi^{(3)}$. The residual fourth- and fifth-order dispersions will then be $\Phi^{(4)} = -3.4\times10^{-7}$ ps^4 and $\Phi^{(5)} = 4.0\times10^{-9}$ ps^5. Our calculations indicate that these residual dispersions, as well as clipping the emission spectrum by the 92-nm transmission band of the stretcher, will increase the transform-limited Gaussian pulse duration (30 fs) to 38 fs. At the same time, since the effects of different orders of dispersion on the shape of ultra-short pulses cancel each other [25], one can use a second-order dispersion detuning $\Delta\Phi^{(2)} = 1.5\times10^{-4}$ ps^2 to partially compensate for the effect of $\Phi^{(4)}$ and a dispersion detuning $\Delta\Phi^{(3)} = -1.1\times10^{-6}$ ps^3 to partially compensate for the effect of $\Phi^{(5)}$, which will reduce the pulse duration to 35.3 fs.

Pulse broadening is accompanied by temporal pulse contrast degradation. To the above residual dispersion values corresponds a contrast of 10^8 over times of ~1 ps. Figure 5 demonstrates how clipping the pulse spectrum by the 92-nm transmission band influences the pulse duration and contrast. It is seen that it takes ~30 ps to reach a contrast of 10^8. According to our estimates, increasing the transmission bandwidth of the stretcher to 113 nm will allow a temporal contrast of 10^8 to be reached in 10 ps, and the minimum pulse duration will decrease to 34.5 fs. To determine the temporal contrast of amplified pulses at the output of the system, additional information is needed about the amplification process, characteristics of the pump light, etc., which is beyond the scope of this paper.

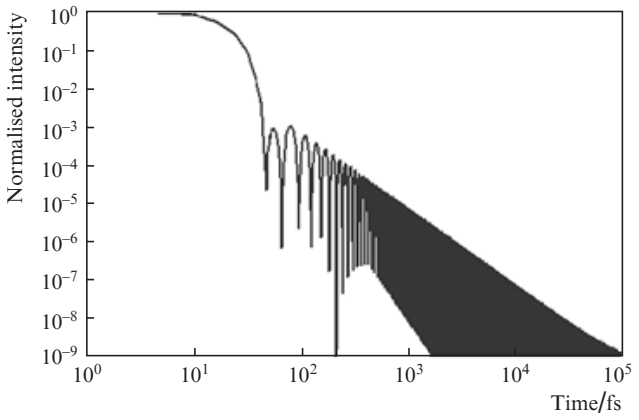

Figure 5. Temporal profile of a 30-fs pulse whose spectrum is clipped by the 92-nm-wide transmission band of the stretcher.

Estimates of the vertical and horizontal angular chirps (angular dispersion) at the stretcher output for light with a 92-nm bandwidth show that, at beam diameters under 8 mm, they do not exceed the diffraction angle.

The results of the above analysis for PEARL allowed us to make a new, eight-pass single-grating stretcher with an Offner triplet based on spherical mirrors (Fig. 6). In this stretcher, we used a diffraction grating 130×130 mm in dimensions with a groove density of 1200 lines mm^{-1}, a concave spherical mirror with a 1200-mm radius of curvature and an aperture of 240×130 mm and a convex spherical mirror with a 600-mm radius of curvature and an aperture of 92×40 mm. The diffraction grating was located 83.3 cm (120–36.7 cm) from the concave mirror.

A beam-expanding telescope increased the Ti:sapphire FMO beam diameter to 8 mm and transferred the beam image from the oscillator output to the stretcher input. The laser beam was incident on the diffraction grating at 43.13° in a horizontal plane situated 5 cm below the principal plane of the stretcher. After being reflected from the grating, it passed through the Offner triplet and again impinged on the grating,

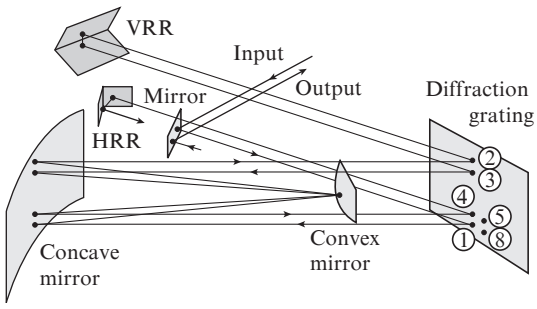

Figure 6. Schematic of light propagation through an eight-pass single-grating Offner stretcher. The circled numbers specify the sequence in which the pulse being chirped impinges on the grating.

but in the upper section in this case, 5 cm above the principal plane. Next, the beam reflected from the grating was shifted 2 cm downwards by the VRR for the next pass through the stretcher (Fig. 6). After the fourth reflection from the diffraction grating, the beam was directed to the HRR, which shifted it by 1.5 cm in a horizontal direction and directed it back to the grating. Accordingly, the beam left the stretcher in the same section where it entered the stretcher.

Measurements of the spectrum of the light that passed through the stretcher showed that the FMO emission spectrum did not become narrower: the measured transmission bandwidth of the stretcher was 92 nm. The total power transmission coefficient of the stretcher was 15%, which resulted from the low efficiency (under 85%) of the diffraction grating.

To ascertain the operational capability of the stretcher, light that passed through it was directed to a single-grating compressor identical in characteristics to that of PEARL in order to minimise the pulse duration. After adjusting the stretcher and compressor using the AA-20DD autocorrelator, we measured the duration of the compressed pulses, which was determined to be ~36 ps. The corresponding intensity autocorrelation trace is presented in Fig. 7.

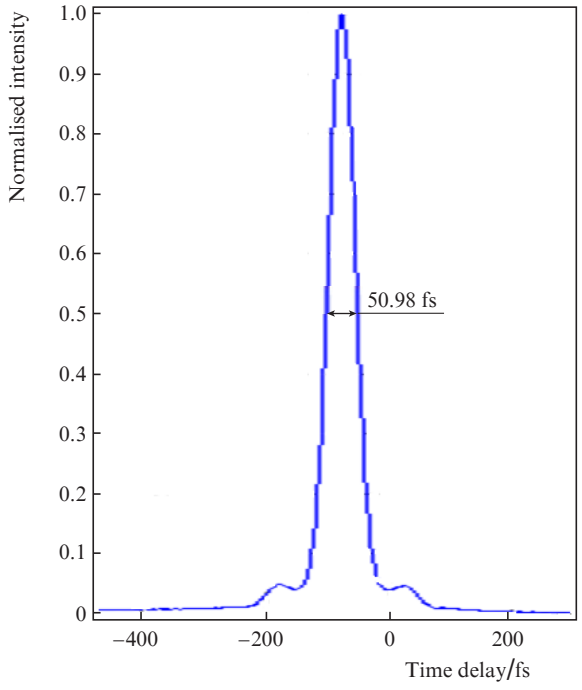

Figure 7. Intensity autocorrelation trace corresponding to a compressed pulse duration of 36 fs.

4. Conclusions

In experiments aimed at compressing femtosecond Ti:sapphire oscillator pulses with a centre wavelength of 910 nm using chirped mirrors, we have obtained 30.3-fs transform-limited pulses.

An unconventional approach based on calculation of a zero-dispersion stretcher has been used to analyse various stretcher configurations for the PEARL laser facility. Using a configuration with an Offner triplet based on spherical mirrors, we have calculated and produced an eight-pass stretcher dispersion-matched to the existing compressor of PEARL. In preliminary pulse compression experiments (without amplification), we obtained ~36-fs pulses.

A transition has been made to a conventional OPCPA scheme in PEARL, in which injected collimated chirped femtosecond oscillator pulses with a centre wavelength of 910 nm are sequentially amplified in three parametric amplifier stages and then sent to the compressor. The 'end-to-end' use of the same light in the stretcher and compressor offers an additional advantage in matching and adjusting elements of these devices, because it can be performed without using parametric amplifiers.

Upgrading the front end of PEARL will ensure the compression of amplified pulses in the compressor to 34–37 fs, which will considerably raise the output peak power of the laser system.

Acknowledgements. We are grateful to A.V. Konyashchenko and A.O. Mavritskii for making the Ti:sapphire laser for the PEARL facility. This work was supported by the Presidium of the Russian Academy of Sciences (Physics and Fundamental Applications of Extreme Laser Radiation Programme) and the RF Ministry of Education and Science (Project No. 14. Z50.31.0007).

References

1. Chu Y., Liang X., Yu L., Xu Y., Xu L., Ma L., Lu X., Liu Y., Leng Y., Li R., Xu Z. *Opt. Express*, **21**, 29231 (2013).
2. Yu T.J., Lee S.K., Sung J.H., Yoon J.W., Jeong T.M., Lee J. *Opt. Express*, **20**, 10807 (2012).
3. Wang Z., Liu C., Shen Z., Zhang Q., Teng H., Wei Z. *Opt. Lett.*, **36**, 3194 (2011).
4. Matras G., Lureau F., Laux S., Casagrande O., Radier C., Chalus O., Caradec F., Boudjemaa L., Simon-Boisson C.A., Dabu R., Jipa F., Neagu L., Dancus I., Sporea D., Fenic C., Grigoriu C. *Proc. CLEO 2013* (San Jose, Cal.: OSA, 2013) CTh5C.5.
5. Yakovlev I.V. *Quantum Electron.*, **44**, 393 (2014) [*Kvantovaya Elektron.*, **44**, 393 (2014)].
6. Kane S., Squier J. *J. Opt. Soc. Am. B*, **14**, 1237 (1997).
7. Zhang Z., Song Y., Sun D., Chai L., Sun H., Wang C. *Opt. Commun.*, **206**, 7 (2002).
8. Yang Q., Guo A., Xie X., Zhang F., Sun M., Gao Q., Li M., Lin Z. *Rev. Laser Eng.*, **36**, 1053 (2008).
9. Leshchenko V.E., Trunov V.I., Pestryakov E.V., Frolov S.A. *Opt. Atmos. Okeana*, **27**, 332 (2014).
10. Lozhkarev V.V., Freidman G.I., Ginzburg V.N., Katin E.V., Khazanov E.A., Kirsanov A.V., Luchinin G.A., Mal'shakov A.N., Martyanov M.A., Palashov O.V., Poteomkin A.K., Sergeev A.M., Shaykin A.A., Yakovlev I.V. *Laser Phys. Lett.*, **4**, 421 (2007).

11. Freidman G.I., Yakovlev I.V. *Quantum Electron.*, **37**, 147 (2007) [*Kvantovaya Elektron.*, **37**, 147 (2007)].
12. Mironov S.Yu., Ginzburg V.N., Gacheva E.I., Silin D.E., Kochetkov A.A., Mamaev Yu.A., Shaykin A.A., Khazanov E.A., Mourou G.A. *Laser Phys. Lett.*, **12**, 025301 (2015).
13. Yakovlev I. *Proc. SPIE Int. Soc. Opt. Eng.*, **9513**, 951308 (2015).
14. Martinez O.E. *IEEE J. Quantum Electron.*, **QE-23**, 59 (1987).
15. Pessot M., Maine P., Mourou G. *Opt. Commun.*, **62**, 419 (1987).
16. Rudd J.V., Korn G., Kane S., Squier J., Mourou G., Bado P. *Opt. Lett.*, **18**, 2044 (1993).
17. Banks P.S., Perry M.D., Yanovsky V., Fochs S.N., Stuart B.C., Zweiback J. *IEEE J. Quantum Electron.*, **36**, 268 (2000).
18. Du D., Squier J., Kane S., Korn G., Mourou G., Bogusch C., Cotton C.T. *Opt. Lett.*, **20**, 2114 (1995).
19. Cheriaux G., Rousseau P., Salin F., Chambaret J.P., Walker B., Dimauro L.F. *Opt. Lett.*, **21**, 414 (1996).
20. Offner A. US Patent 3748015 (1973).
21. Weiner A.M. *Rev. Sci. Instrum.*, **71**, 1929 (2000).
22. Weiner A.M., Heritage J.P., Kirschner E.M. *J. Opt. Soc. Am. B*, **5**, 1563 (1988).
23. Weiner A.M. *Opt. Commun.*, **284**, 3669 (2011).
24. Druon F., Hanna M., Lucas-Leclin G., Zaouter Y., Papadopoulos D., Georges P. *J. Opt. Soc. Am. B*, **25**, 754 (2008).
25. Bagnoud V., Salin F. *IEEE J. Sel. Top. Quantum Electron.*, **4**, 445 (1998).